Pressure/temperature and volume mixing ratio retrievals for the Atmospheric Chemistry Experiment (ACE)

Chris Boone* and Peter Bernath
Department of Chemistry, University of Waterloo

ABSTRACT

Scisat-1, otherwise known as the Atmospheric Chemistry Experiment, is a satellite mission designed for remote sensing of the Earth's atmosphere using occultation spectroscopy. The primary goal of the mission is to investigate the chemical and dynamical processes that govern ozone distribution in the stratosphere and upper troposphere. It has been developed under the auspices of the Canadian Space Agency and is scheduled for launch in December of 2002. The primary instrument on board Scisat-1 is a high resolution Fourier transform spectrometer (FTS) operating in the infrared. Pressure and temperature as a function of altitude will be determined from the FTS measurements through analysis of carbon dioxide absorption. Volume mixing ratio (vmr) profiles will be retrieved for more than thirty molecules of atmospheric interest. Both the pressure/temperature and vmr retrievals use non-linear least squares Global Fit type approaches. For the pressure/temperature analysis, several variations are being developed; the choice of which version to implement depends on the quality of the pointing information obtained from the satellite. In the case of poor pointing knowledge, tangent height separations between measurements will be determined directly from the FTS data (simultaneously with the pressure and temperature determination) through the imposition of hydrostatic equilibrium.
Keywords: remote sensing, occultation spectroscopy, geophysical parameter retrieval

1. INTRODUCTION

The Atmospheric Chemistry Experiment (ACE) is the first in a planned series of small science satellites to be flown by the Canadian Space Agency. Scheduled for launch in December of 2002, ACE will perform remote sensing of the Earth's atmosphere from low Earth orbit (650 km altitude). The ACE mission will contribute to the investigation of ozone depletion mechanisms, with a focus on northern high-latitudes. The planned duration of the mission is two years.

The primary instrument on board the satellite is a Fourier transform spectrometer (FTS) operating between 2 and 13 microns with an unapodized resolution of 0.02 cm^{-1}. Also on board is a UV/Visible spectrometer operating between 0.285 and 1.03 microns with a resolution of 1 to 2 nm.

The measurement technique to be used for the mission is solar occultation, the geometry of which is depicted in Fig. 1.

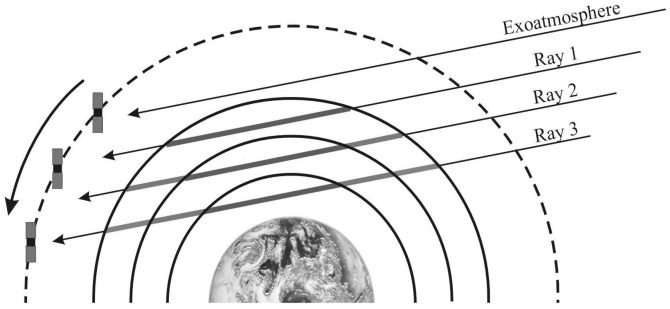

Fig. 1: Solar occultation geometry

*cboone@uwaterloo.ca; phone (519) 888-4567 x2723; fax (519) 746-0435; http://www.ace.uwaterloo.ca; Department of Chemistry, University of Waterloo, Waterloo, Ontario, Canada, N2L 3G1

Earth Observing Systems VII, William L. Barnes, Editor,
Proceedings of SPIE Vol. 4814 (2002) © 2002 SPIE · 0277-786X/02/$15.00

Over the course of an occultation event (i.e., a sunrise or a sunset in the satellite's frame of reference), the instruments take a series of measurements, where each measurement corresponds to a different ray path of sunlight through the Earth's atmosphere. Exoatmospheric measurements (solar measurements with no intervening atmosphere) are used as reference spectra, making the ACE instruments self-calibrating.

Fig. 2 shows a set of (calibrated) FTS measurements taken over one occultation by the Atmospheric Trace Molecule Spectroscopy (ATMOS) mission flown by NASA on the space shuttle.[1] Altitude labels on the left of Fig. 2 correspond to the altitudes of closest approach to the Earth for the solar rays being measured, otherwise known as *tangent heights.* The ACE-FTS instrument will measure similar sets of spectra, with a tangent height spacing of 3 to 4 km.

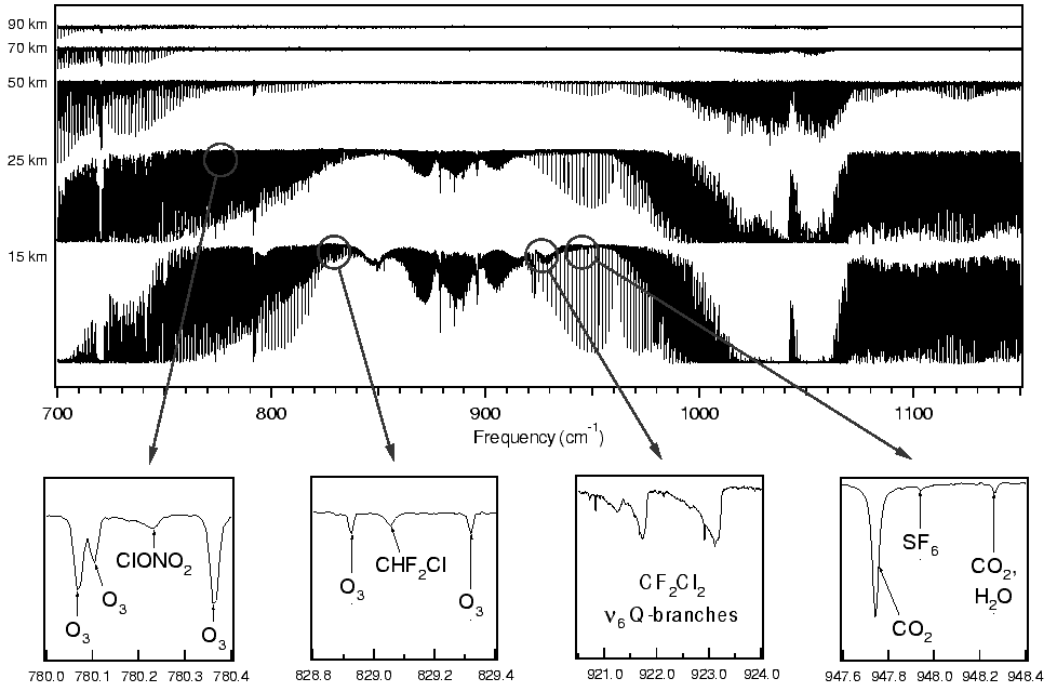

Fig. 2: Spectra from an ATMOS occultation (courtesy of Curtis Rinsland)

2. ANALYSIS

Rather than analyzing the entire spectrum at once (a daunting prospect), only small (~0.03 to 1 cm^{-1} wide) portions of the spectrum containing the most pertinent information are analyzed. These small portions of the spectrum, together with the associated ranges of tangent heights to be included in the analysis, are known as *microwindows*.

Interpretation of the ACE-FTS data begins with the calculation of synthetic spectra using what is known as the *forward model*. In the forward model, a solar ray is traced along the path it would follow through the atmosphere, including the effects of refraction. Using assumed altitude profiles for pressure, temperature, and the volume mixing ratios (vmrs) of atmospheric constituents, the transmittance of light as a function of frequency (i.e., the spectrum) over the entire path is then calculated. Volume mixing ratios for the molecules of interest, pressure, and temperature are thus parameters in the model than can (in principle) be determined from a nonlinear least squares fit. It is convenient to divide the analysis into two steps, whereby pressure and temperature are determined first, and then the vmrs for the molecules of interest are determined in a subsequent step

2.1 Pressure/temperature

There are (at least) two independent pieces of information in FTS spectra where individual lines are well resolved: the relative intensities of different lines and the absolute intensities of the lines. In principle, the shape of a spectral line also contains further information, but such information will be minimal at best for the ACE-FTS and is therefore ignored.

There are a number of temperature-related factors that determine the absorption cross section for a particular line. One significant factor—and one that can vary the most dramatically from line to line—is the lower state population for the associated molecular transition. The population in the lower state has an exponential dependence on the energy of the state.[2] Thus, the relative intensities of lines having different lower state energies gives a fairly direct measure of temperature.

The second piece of independent information, the absolute intensities, can be used to determine one other parameter (i.e., other than temperature), but there is more than one variable remaining: pressure, density, and the vmrs of atmospheric constituents. In the case of poor pointing knowledge for the satellite, the geometry of the measurement itself becomes an unknown parameter. Because there is insufficient information to determine all the quantities of interest, constraints must be introduced to reduce the number of independent parameters. For example, by imposing the constraint of the ideal gas law, density can be expressed as a function of pressure and temperature, thereby reducing the number of independent parameters by one.

Another available constraint is that of hydrostatic equilibrium, which is described by the following expression:

$$\frac{dP}{dz} = -g\rho = \frac{-gm_a P}{kT}, \tag{1}$$

where P is pressure, z is altitude, g is acceleration due to gravity at altitude z, ρ is density at that altitude, m_a is the average molecular mass, k is the Boltzmann constant, and T is the temperature at altitude z. Note that the ideal gas law was used to expand the right hand side in Eq. 1, removing density from the equation.

The most appropriate approach to use for imposing the constraint of hydrostatic equilibrium depends on whether or not the satellite provides accurate pointing knowledge. The quality of pointing knowledge that will be derived from Scisat-1 has yet to be established, and so algorithms were developed for both the good pointing knowledge and poor pointing knowledge cases.

2.1.1 Poor pointing knowledge

Rearranging and integrating Eq. 1 yields the following expression:

$$\int_{P_1}^{P_2} \frac{dP}{P} = \ln\left(\frac{P_2}{P_1}\right) = \frac{-m_a}{k}\int_{z_1}^{z_2} \frac{g}{T}\,dz, \tag{2}$$

where P_1 is the pressure at altitude z_1, and P_2 is the pressure at altitude z_2. Note that the average molecular mass has been taken to be constant as a function of altitude, which will lead to slight errors for altitudes above about 80 km.

Solving the integral on the right hand side of Eq. 2 requires knowledge of the variations as a function of altitude for both g and T. In fitting for temperature, it is more convenient to work in terms of 1/T. A piecewise quadratic variation is assumed for 1/T; i.e., over a short altitude range, it is assumed that the variation of 1/T with altitude can be represented by a quadratic expression:

$$\frac{1}{T}(z) = \frac{(z-z_2)(z-z_3)}{(z_1-z_2)(z_1-z_3)}\frac{1}{T_1} + \frac{(z-z_1)(z-z_3)}{(z_2-z_1)(z_2-z_3)}\frac{1}{T_2} + \frac{(z-z_1)(z-z_2)}{(z_3-z_1)(z_3-z_2)}\frac{1}{T_3}, \tag{3}$$

where z_1, z_2, and z_3 are tangent heights corresponding to the measurements, and T_1, T_2, and T_3 are the temperatures at

those altitudes. The values of 1/T at the tangent heights (i.e., $1/T_1$, $1/T_2$, etc.) are parameters that are determined from the least squares fit.

In the case of poor pointing knowledge, care must be taken in expressing the altitude variation of g in Eq. 2. The ACE mission will receive a new data set on average every 45 minutes. Therefore, processing time is a major consideration. The least squares analysis process requires the derivatives of the calculated signal with respect to each of the model parameters. Calculating these derivatives analytically is much faster than performing the calculations numerically. Ideally, then, one would like to generate an analytical solution to the integral on the right hand side of Eq. 2. The variation of g with altitude can be expressed as follows:

$$g(z,\lambda) = g_o(\lambda)\frac{R_{eff}^2(\lambda)}{\left(R_{eff}(\lambda)+z\right)^2} \approx g_o(\lambda)\left(1-\frac{2z}{R_{eff}(\lambda)}\right), \tag{4}$$

where λ represents latitude, R_{eff} is the effective radius of the Earth at that latitude (calculated from an oblate spheroid model for the effective sea level surface), and $g_o(\lambda)$ is the acceleration due to gravity at sea level.

The separation between tangent heights (e.g., z_1-z_2, or z_1-z_3) can be calculated from the expression in Eq. 2 if the pressures and temperatures at the tangent heights are known. The exact solution to the integral on the right hand side of Eq. 2 (assuming the quadratic variation for 1/T in Eq. 3 and the first expression for g in Eq. 4) is straightforward but makes solving for the tangent height separations impossible. However, by using the approximate relation for g (i.e., the second expression in Eq. 4), the integral on the right hand side of Eq. 2 can be evaluated using Simpson's rule,[3] which is exact for expressions up to cubic, and analytical solutions for tangent height separations become possible.

The first step is to evaluate Eq. 2 between z_1 and z_2. In order to make use of Simpson's rule, this involves evaluating 1/T at $z = 0.5*(z_1+z_2)$ using the expression in Eq. 3. With some minor rearrangement, the resulting equation can be expressed in terms of (z_1-z_2) and (z_1-z_3):

$$\begin{aligned}\frac{6k}{g_o(\lambda)m_a}\ln\left(\frac{P_2}{P_1}\right) &= x\left[\left(2+\frac{y-x}{y}\right)\frac{1}{T_1}+\left(2+\frac{y}{y-x}\right)\frac{1}{T_2}-\frac{x^2}{y(y-x)}\frac{1}{T_3}\right] \\ &-\frac{2x}{R_{eff}}\left[\left(2z_1-\frac{1}{2}x\right)\frac{1}{T_1}+\left(2z_1-\frac{3}{2}x\right)\frac{1}{T_2}+\left(z_1-\frac{1}{2}x\right)\left(\frac{y-x}{y}\frac{1}{T_1}+\frac{y}{y-x}\frac{1}{T_2}-\frac{x^2}{y(y-x)}\frac{1}{T_3}\right)\right],\end{aligned} \tag{5}$$

where $x\equiv(z_1-z_2)$ and $y\equiv(z_1-z_3)$. Note that z_1 is assumed known accurately.

If x were known in Eq. 5, one could solve for y, but that would involve finding the solution to a quartic equation (not the most attractive option). A similar expression to Eq. 5 can be written for going from z_1 to z_3. Combining this expression with the one in Eq. 5 leads to a more reasonable cubic equation in y:

$$\begin{aligned}&\frac{1}{R_{eff}}\left(\frac{1}{T_1}-\frac{1}{T_2}\right)y^3+\left[\left(\frac{1}{T_1}-\frac{1}{T_2}\right)\left(1-\frac{2z_1}{R_{eff}}\right)-\frac{x}{R_{eff}}\left(\frac{3}{T_3}+\frac{2}{T_1}+\frac{1}{T_2}\right)\right]y^2+ \\ &\left[\frac{-6k}{g_o(\lambda)m_a}\ln\left(\frac{P_2}{P_1}\right)+2x\left(\frac{1}{T_2}-\frac{1}{T_3}\right)\left(1-\frac{2z_1}{R_{eff}}\right)+\frac{x^2}{R_{eff}}\left(\frac{3}{T_2}+\frac{2}{T_1}+\frac{1}{T_3}\right)\right]y+ \\ &x\left(\frac{6k}{g_o(\lambda)m_a}\ln\left(\frac{P_3}{P_1}\right)\right)+x^2\left(\frac{1}{T_3}-\frac{1}{T_1}\right)\left(1-\frac{2z_1}{R_{eff}}\right)+\frac{x^3}{R_{eff}}\left(\frac{1}{T_3}-\frac{1}{T_1}\right)=0\end{aligned} \tag{6}$$

So, if z_1 is known accurately, and x (i.e., z_1-z_2) is known, then one can solve for y (i.e., z_1-z_3) from Eq. 6, taking the smallest positive (and real) value of the three possible solutions. Imposing the constraint of hydrostatic equilibrium in Eq. 2 *plus* defining a reference pressure at some known altitude allows tangent heights to be written in terms of pressure and temperature at the measurement tangent heights, thereby reducing the number of independent unknown parameters.

With the reductions achieved by imposing the constraints of the ideal gas law and hydrostatic equilibrium, there are still three unknowns (pressure, temperature, and the vmrs of atmospheric constituents), and the data analysis can only reliably support two unknowns, as was discussed previously. The simplest solution is to analyze one molecule (or a small set of molecules) for which the vmr is well known. The vmr can then be fixed in the analysis, leaving only two independent parameters. Note that the variation of the vmr as a function of altitude must also be well known in order to avoid biasing the results. The obvious candidate for this approach is CO_2, whose vmr profile is shown in Fig. 3.

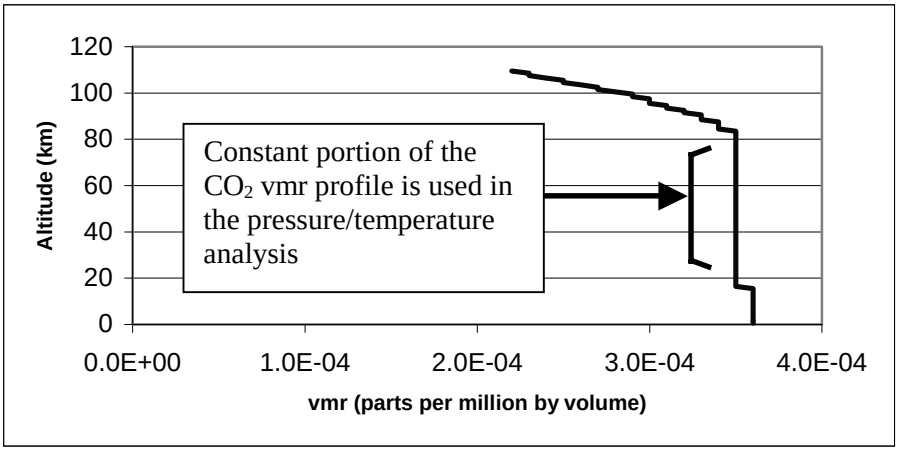

Fig. 3: CO_2 vmr profile, circa 1994

In the middle atmosphere (~15 to ~80 km), CO_2 is perfectly mixed and therefore has a constant vmr. It is in this altitude region that the approach described above can be employed, particularly since the value of the CO_2 vmr in this region is well known. Unfortunately, above 80 km or so, the variation of CO_2 vmr with altitude is not well known and cannot be used to determine geometry.

Atmospheric measurements for the ACE mission will extend up to 100 km in altitude. For efficiency of processing time, the entire altitude range (10 to 100 km) is analyzed at once. The altitude range is divided into two regions, high altitudes and low altitudes, where the crossover altitude (the dividing line between the two regions) is taken to be the measurement tangent height nearest to 70 km. When air descends in the winter vortex region, this crossover altitude may need to be chosen somewhat lower.[4]

For altitudes above the crossover point, there is no alternative but to assume good pointing knowledge. However, this is not a fatal limitation, because problems with pointing knowledge (e.g., deteriorated performance of suntracker, refractive distortion of solar image, etc.) are most significant at lower altitudes. For higher tangent heights, good pointing knowledge can be achieved from relatively simple geometry calculations (assuming accurate characterization of the satellite orbit). Thus, in the temperature/pressure retrievals for the case of poor pointing knowledge, tangent heights are fixed at high altitudes (to the best values that can be obtained, bad as they may be) down to the crossover measurement (the measurement nearest to 70 km). The tangent height for the first measurement below the crossover must also be fixed, because of the need to know x in Eq. 6. The tangent height separations for measurements below the crossover are then calculated using Eq. 6. The calculation always employs three *successive* measurements, with the tangent height determined in one step used to calculate the value of x (in Eq. 6) required for the next step, working downward from the crossover point to the lowest measurement used in the analysis.

Above the crossover, tangent heights are fixed, pressure is calculated from Eq. 2 (using the exact form for g in Eq. 4 rather than the approximate form, because one does not need to solve for tangent height separations), and the parameters

to be determined in the least squares fit are 1/T and CO_2 vmr at the tangent heights. For the crossover measurement and below, CO_2 vmr is fixed to its known value, tangent height separations are calculated from Eq. 6 (other than for the first separation below the crossover), and the parameters are 1/T and P at the tangent heights. In both cases, two parameters are determined per measurement, the maximum available information content.

Forward model calculations are performed on a standard grid, defined by 1 km thick concentric shells, where physical properties (pressure, temperature, vmr) within a shell are assumed constant. Because values of the parameters are only defined at the measurement tangent heights, they must be interpolated onto the standard grid. Eq. 3 is used to interpolate 1/T onto the standard grid for both the low and high altitude regions. At high altitudes, a similar piecewise quadratic expression is used to interpolate CO_2 vmr:

$$vmr(z) = \frac{(z-z_2)(z-z_3)}{(z_1-z_2)(z_1-z_3)} vmr(z_1) + \frac{(z-z_1)(z-z_3)}{(z_2-z_1)(z_2-z_3)} vmr(z_2) + \frac{(z-z_1)(z-z_2)}{(z_3-z_1)(z_3-z_2)} vmr(z_3). \quad (7)$$

Eq. 2, the equation for hydrostatic equilibrium, is used to interpolate P onto the standard grid in both the low and high altitude regions.

Recall that a reference pressure at some altitude is required. This is introduced by scaling all of the calculated pressures (i.e., the values interpolated onto the standard grid) to ensure a match at the appropriate altitude. This is an equivalent operation to shifting all of the measurements in altitude, except scaling the pressure preserves the values fixed for the tangent heights at high altitude.

2.1.2 Good pointing knowledge

Pressure/temperature retrievals become much simpler when good pointing information is obtained from the satellite. The analysis software uses the same general structure as for the poor pointing knowledge case: the atmosphere is divided into two regions, high and low altitude. The analysis for high altitudes is exactly the same, while the analysis procedure for low altitudes differs significantly.

At low altitudes, parameters for the least squares fit will again include 1/T at each measurement tangent height. The pressure at one altitude must be included as a parameter in the fit (or explicitly fixed). The ACE analysis software takes the pressure at the crossover measurement as an adjustable parameter. There is no direct measure of the tangent heights themselves from a satellite, but rather the angles in which the instruments were pointing. Tangent heights and tangent pressures for the measurements below the crossover are determined from an iterative process.

$$z_t \approx r_s \sin\theta \left(1 - \alpha \frac{P_t}{T_t}\right) - R_{eff}, \quad (8)$$

where r_s is the distance of the satellite from Earth centre, θ is the solar zenith angle (the angle between the satellite-Earth plumb line and the instrument pointing direction), and the subscript t refers to the value of the particular quantity at the tangent point. The quantity α varies slowly as a function of wavenumber, but dispersion is so small in the infrared that it is taken to be a constant, calculated for a wavenumber near the centre of the ACE region (i.e., at 2400 cm^{-1}), for which it has the value 0.078574065.

The iterative method for finding z_t and P_t from Eq. 8 begins by calculating z_t for $P_t = 0$. The pressure is then calculated at this height using Eq. 2, integrating down from the next highest tangent point, where the pressure and tangent height are both assumed known. A new value for z_t is then calculated from Eq. 8, P_t is recalculated, and so on until convergence. This procedure is propagated downward from the crossover point (recall that the pressure at the crossover point is a parameter in the least squares fit), finding tangent height and tangent pressure for each measurement. Above the crossover point, the effects of refraction are negligible, and the tangent heights can therefore be calculated from geometry (Eq. 8 with P_t set to zero).

At and below the crossover, CO_2 vmr is fixed, z_t and P_t are calculated from a combination of Eqs. 2 and 8, and 1/T at the measurement tangent heights are the parameters to be determined in the least squares fit. Note that the extra information content (recall that the analysis can support two parameters per measurement) constrains the fit enough that imposing a reference pressure is not necessary. Note also that the extra information content means that CO_2 vmr could be retrieved at lower altitudes (just as it is at the higher altitudes). Measuring the small geographical variations expected in CO_2 vmr would be a very interesting result.

2.1.3 Pressure/temperature microwindows

Isolating the analysis to CO_2 requires the selection of microwindows that contain minimal spectral contamination from other atmospheric constituents. The microwindow set needs to contain lines with a broad range of lower state energies in order to accurately retrieve temperature. Software development made use of the existing ATMOS data set as a test case for analysis. The ATMOS instrument did not cover as broad a spectral range as will the ACE-FTS instrument, but had a number of smaller frequency ranges. Thus, CO_2 microwindow sets to be used in pressure/temperature retrievals were generated for the ATMOS frequency ranges. The ACE CO_2 microwindow set will be a combination of these sets.

The criteria for microwindow selection included: less than one percent spectral contamination under nominal conditions (usually much less than that), a portion of baseline in each window, and a broad distribution of lower state energies at every altitude. At any altitude, there is at least one line with lower state energy less than 50 cm^{-1}, at least one line with lower state energy between 50 and 150 cm^{-1}, at least line with lower state energy between 150 and 250 cm^{-1}, and so on, in bins of width 100 cm^{-1} as high in lower state energy as possible (up to ~ 3000 cm^{-1} for some altitudes). The choice of bins was fairly arbitrary, but was designed to give enough lines to provide decent statistics.

The CO_2 pressure/temperature retrieval microwindows are listed in Tables 1 through 3.

2.2 Vmr retrievals

Pressure, temperature, and tangent heights are all established in the pressure/temperature retrieval stage. Least squares fitting parameters for vmr retrievals are the vmrs at measurement tangent heights. Interpolation onto the standard 1 km grid is performed using the expression in Eq. 7, piecewise quadratic. For optimization of processing speed, derivatives with respect to the fitting parameters are once again calculated analytically.

Microwindow sets are selected (where possible) to minimize spectral contamination from other species. As such, most gases are retrieved independently. For some heavier molecules, such as N_2O_5 and CFC-11, which have broad absorption features, it is not possible to find microwindows clear of interferences. Thus, a multiple molecule approach has been developed for ACE, whereby several molecules can be analyzed at the same time. The molecule of interest and the interferers are retrieved simultaneously, and then information on the interferers is discarded. The multiple molecule approach also has benefits for CO, allowing retrieval down to lower altitudes than would otherwise be possible.

3. RESULTS

Software development used test retrievals on both synthetic spectra and ATMOS spectra to ensure internal consistency and stability. Much effort was made to ensure the stability of the software with respect to the quality of initial guess (i.e., that it would converge to the same result for a broad range of initial guesses, including poor guesses). Fig. 4 shows the errors in pressure and temperature for a particular pressure/temperature retrieval from a set of synthetic spectra. Note that the “true” values are known only because we are dealing with synthetic spectra. For real spectra, the deviation from truth will be unknown. Errors in temperature exceed 30 K, and errors in pressure exceed 40 percent. The initial guess was taken to be the result from an ATMOS occultation, to ensure that it was physically reasonable. Initial guesses for ACE will come from data extracted from meteorological services (in part), and should be much closer to truth than the situation in Fig. 4.

#	center (cm-1)	width (cm-1)	z_{low} (km)	z_{high} (km)	#	center (cm-1)	width (cm-1)	z_{low} (km)	z_{high} (km)
1	1890.40	0.30	20	32	42	2348.00	0.40	66	90
2	1896.26	0.30	33	42	43	2353.72	0.65	70	90
3	1899.17	0.35	32	45	44	2361.37	0.50	85	100
4	1902.12	0.40	41	50	45	2369.14	0.45	85	100
5	1905.10	0.30	32	53	46	2371.43	0.45	83	100
6	1909.45	0.40	34	54	47	2373.67	0.45	80	100
7	1911.00	0.45	35	54	48	2375.81	0.45	80	100
8	1920.11	0.45	30	45	49	2377.85	0.45	74	100
9	1924.76	0.45	38	50	50	2379.78	0.45	90	100
10	1929.35	0.45	30	38	51	2380.72	0.45	72	100
11	1934.77	0.30	30	41	52	2381.62	0.45	85	100
12	1941.12	0.40	20	30	53	2382.50	0.45	65	95
13	1950.70	0.30	24	32	54	2384.19	0.45	58	90
14	1966.87	0.30	28	35	55	2385.00	0.45	55	88
15	1968.64	0.30	22	32	56	2385.80	0.45	55	82
16	1970.12	0.30	20	33	57	2386.53	0.45	54	78
17	1975.08	0.40	10	22	58	2387.26	0.40	50	76
18	2047.56	0.30	50	62	59	2387.96	0.40	50	73
19	2050.52	0.40	53	62	60	2388.64	0.40	45	71
20	2053.55	0.35	54	70	61	2389.29	0.40	40	68
21	2055.09	0.35	54	65	62	2389.92	0.40	37	65
22	2058.27	0.40	60	70	63	2390.52	0.40	30	63
23	2062.87	0.40	60	70	64	2391.15	0.40	30	60
24	2214.70	0.30	45	51	65	2391.70	0.40	32	55
25	2217.16	0.40	43	50	66	2392.18	0.40	32	53
26	2226.65	0.35	40	54	67	2392.62	0.35	25	50
27	2229.78	0.30	40	55	68	2412.47	0.35	21	40
28	2237.32	0.40	50	62	69	2620.84	0.45	10	20
29	2240.01	0.35	45	65	70	2623.71	0.40	10	30
30	2242.82	0.40	46	65	71	2629.50	0.40	10	24
31	2247.63	0.50	62	80	72	3204.76	0.45	10	24
32	2250.19	0.40	40	60	73	3206.41	0.40	10	23
33	2251.79	0.55	62	80	74	3211.33	0.40	10	24
34	2251.92	0.30	45	55	75	3213.00	0.40	10	24
35	2252.42	0.40	45	70	76	3301.57	0.40	10	20
36	2258.40	0.45	50	74	77	3304.70	0.40	10	22
37	2274.07	0.30	50	70	78	3306.22	0.35	12	28
38	2307.65	0.50	65	85	79	3309.46	0.40	24	30
39	2328.62	0.80	90	100	80	3312.63	0.40	24	32
40	2345.75	0.80	90	100	81	3314.15	0.35	23	34
41	2346.88	0.50	70	90	82	3318.99	0.30	24	35

Table 1: CO_2 microwindows for 1550 to 3350 cm^{-1}

#	center (cm-1)	width (cm-1)	z_{low} (km)	z_{high} (km)	#	center (cm-1)	width (cm-1)	z_{low} (km)	z_{high} (km)
1	3204.76	0.45	10	24	31	3563.20	0.40	30	50
2	3206.41	0.40	10	23	32	3571.95	0.45	32	50
3	3211.33	0.40	10	24	33	3589.33	0.40	48	72
4	3213.00	0.40	10	20	34	3591.10	0.30	43	50
5	3301.57	0.40	10	17	35	3592.27	0.30	42	62
6	3304.70	0.40	10	29	36	3609.70	0.40	67	85
7	3306.22	0.35	12	30	37	3611.73	0.30	40	49
8	3314.15	0.35	23	32	38	3618.70	0.30	40	50
9	3318.99	0.30	24	34	39	3631.85	0.40	65	85
10	3344.77	0.30	18	32	40	3634.35	0.40	62	85
11	3349.50	0.40	25	33	41	3637.77	0.35	60	85
12	3354.10	0.35	33	40	42	3638.92	0.40	55	85
13	3358.68	0.30	28	45	43	3644.22	0.40	50	70
14	3367.88	0.30	24	42	44	3645.63	0.30	28	50
15	3369.47	0.30	20	38	45	3654.05	0.30	29	55
16	3377.03	0.30	17	24	46	3658.57	0.35	45	65
17	3378.62	0.28	10	22	47	3663.88	0.40	58	73
18	3475.28	0.30	30	40	48	3666.00	0.40	65	75
19	3477.00	0.35	22	40	49	3668.20	0.40	70	77
20	3487.53	0.40	30	38	50	3669.62	0.35	50	58
21	3493.15	0.40	38	55	51	3670.35	0.40	70	81
22	3496.93	0.35	42	60	52	3671.60	0.30	40	53
23	3515.90	0.30	22	30	53	3672.45	0.40	55	85
24	3518.05	0.30	40	70	54	3673.40	0.30	53	60
25	3521.82	0.30	34	43	55	3676.65	0.40	72	85
26	3532.78	0.30	25	49	56	3676.90	0.30	49	56
27	3534.62	0.35	48	67	57	3685.20	0.40	50	65
28	3547.53	0.45	45	58	58	3697.26	0.30	49	70
29	3551.46	0.35	50	65	59	3724.45	0.40	70	85
30	3560.41	0.30	40	50	60	3731.00	0.35	65	85

Table 2: CO_2 microwindows for 3200 to 4100 cm^{-1} (note some overlap with Table 1)

#	center frequency (cm-1)	width (cm-1)	lower altitude (km)	upper altitude (km)
1	810.93	0.30	12	40
2	812.40	0.30	12	40
3	820.23	0.30	12	30
4	927.00	0.40	12	38
5	929.00	0.40	12	40
6	936.80	0.40	12	45
7	952.88	0.35	24	40

Table 3: CO_2 microwindows below 1000 cm^{-1}

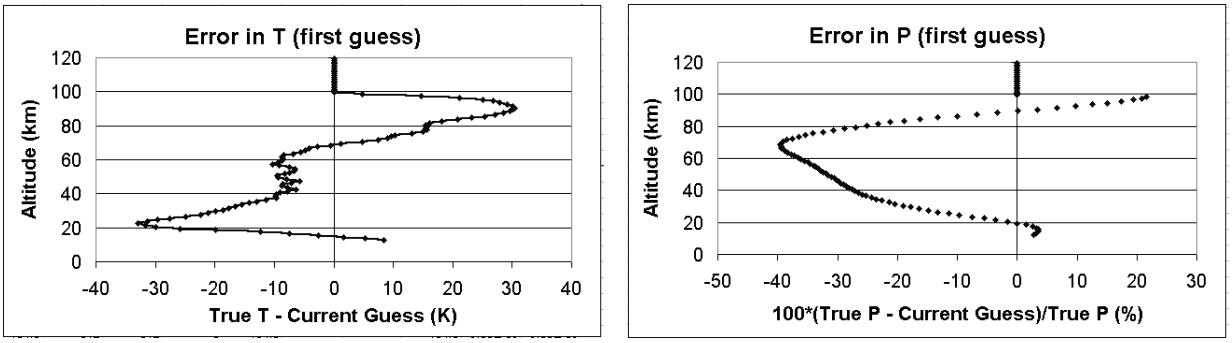

Fig 4: Error in T and P for the first guess in a retrieval from synthetic spectra

The results from the least squares fit for the case of poor pointing knowledge are shown in Fig. 5. Convergence was achieved after 7 iterations. Tangent heights are reproduced to within about 15 m, temperature to within 0.15 K, and pressures to within 0.15%. Note that the synthetic spectra used in the analysis were noise-free. The errors in Fig. 5 are negligible, and would in fact get even smaller if the convergence criterion (χ^2 changing by less than 1 part in 10^4) were made even stricter.

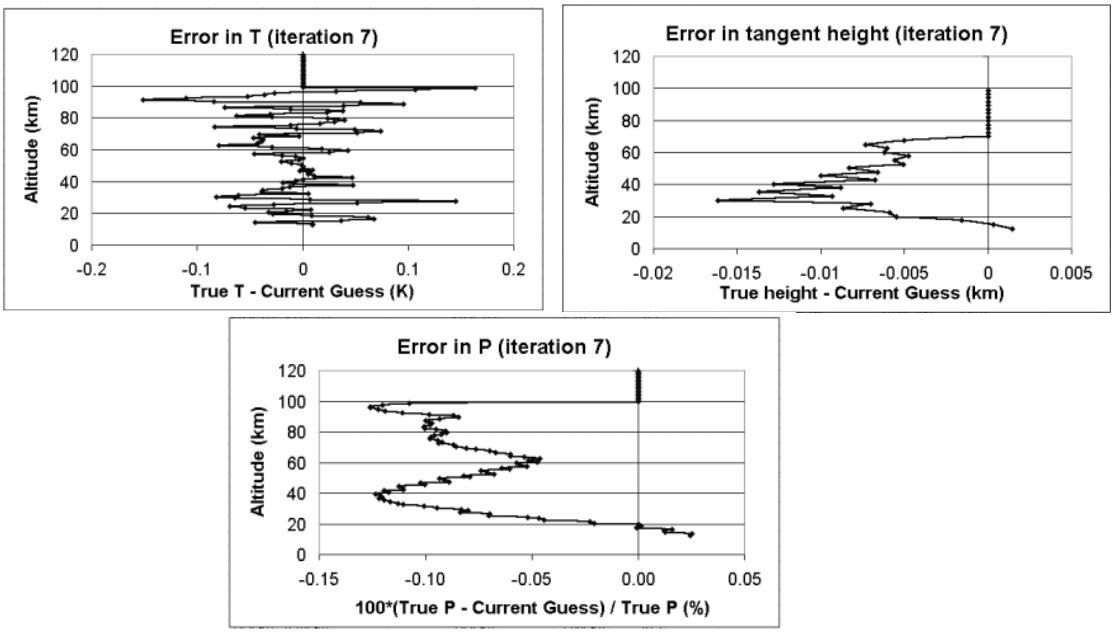

Fig 5: Least squares fitting results, poor pointing knowledge case

Tangent height errors for the same synthetic spectra, and the same initial guess, in the case of good pointing knowledge are shown in Fig. 6. Results for temperature and pressure (not shown) are essentially the same as the results in Fig. 5. As might be expected, the errors in tangent heights are much smaller in the case of good pointing knowledge, less than 4 meters. In the case of bad pointing knowledge, there were contributions to the error from temperature and pressure, while in the case of good pointing knowledge the errors come mostly from approximations used in incorporating the refraction model into the analysis procedure. Note that the case of good pointing knowledge converged much faster, taking four iterations instead of seven.

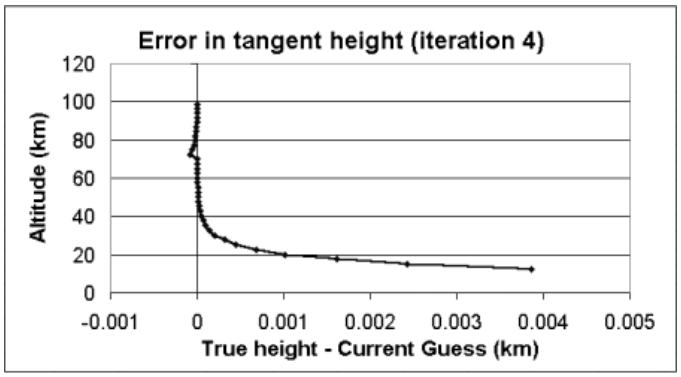

Fig. 6: Tangent height errors for pressure/temperature retrieval on synthetic spectra (good pointing knowledge)

The results for a particular ATMOS occultation are shown in Fig. 7. The occultation is sunset #4 of ATLAS-3, the ATMOS mission that flew in November 1994. Fig. 7 shows the retrieved temperature profile for this occultation using the ACE software and microwindows, along with the temperature profile used in the ATMOS version 3 data processing. The version 3 result is much smoother, but the smoothness was actually enforced by the retrieval process.[5] Agreement between the two results is very good, with the ATMOS result resembling a smoothed or averaged version of the current result. Other than the oscillations at the lowest altitudes, the deviations of the current result from the ATMOS result are physically reasonable. The observed thermal structure is consistent (in altitude and amplitude) with phenomena known as mesospheric inversion layers, often observed with lidar techniques.[6] Similar structure is observed in results for other occultations, but not in all occultations. The oscillations at low altitudes (below 20 km) could be due to a lack of lines with very high lower state energy for this altitude region (all such available lines are saturated). This is under investigation.

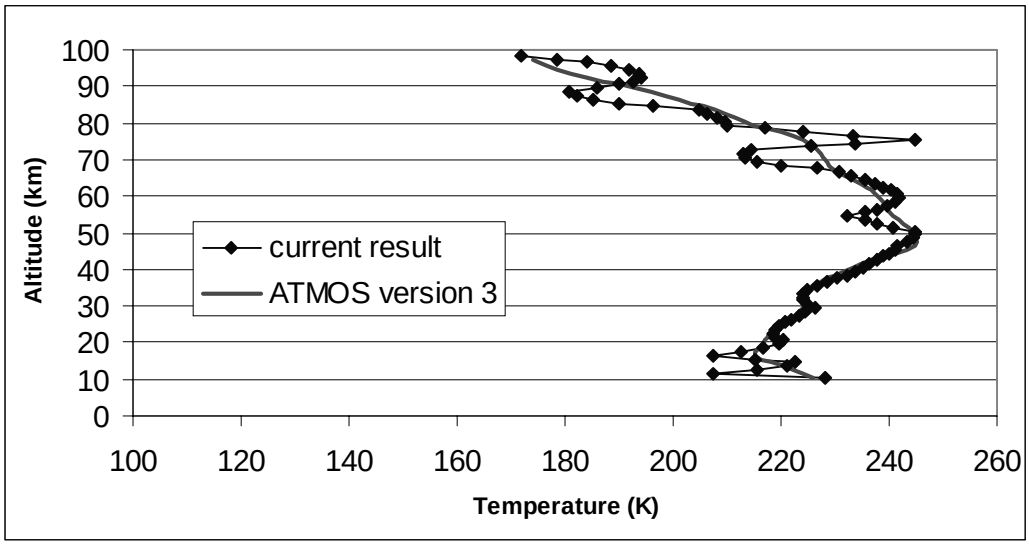

Fig 7: Retrieved temperature profile for sunset #4 of ATMOS ATLAS-3

Vmr retrievals were performed (with synthetic and ATMOS data) for all of the baseline molecules for the ACE mission: O_3, H_2O, CH_4, N_2O, NO_2, NO, HNO_3, N_2O_5, $ClONO_2$, HCl, CCl_2F_2, CCl_3F, HF, and CO. The results for ATMOS data were consistent with previous (ATMOS version 2 and version 3) retrieval results for the same spectra. Results for many other non-baseline molecules have also been retrieved from the ATMOS data set.

4. CONCLUSIONS

Analysis software is currently in place for all aspects of ACE retrievals. Final optimizations for processing speed remain to be implemented. All software is extremely stable with respect to initial guess. Algorithms have been tested using synthetic spectra and receive very good results, but an extensive software validation campaign remains to be performed.

ACKNOWLEDGMENTS

Thanks to the Canadian Space Agency and to NSERC for funding.

REFERENCES

1. M.C. Abrams, M.R. Gunson, A.Y. Chang, C.P. Rinsland, and R. Zander, "Remote sensing of the Earth's atmosphere from space with high-resolution Fourier-transform spectroscopy: development and methodology of data processing for the Atmospheric Trace Molecule Spectroscopy experiment", Applied Optics, **35**, 16, pp 2774-2786, 1996.
2. C.L. Tien and J.H. Lienhard, *Statistical Thermodynamics*, Holt, Rinehart, and Winston Inc., New York, 1971.
3. W.H. Press, S.A. Teukolsky, W.T. Vetterling, and B.P. Flannery, *Numerical Recipes in Fortran 2nd Edition*, Cambridge University Press, New York, 1992.
4. R.G. Roble, "On the feasibility of developing a global atmospheric model extending from the ground to the exosphere", Geophysical Monograph 123, American Geophysical Union, 2000.
5. G.P. Stiller, M.R. Gunson, L.L. Lowes, M.C. Abrams, O.F. Raper, C.B. Farmer, R. Zander, and C.P. Rinsland, "Stratospheric and mesospheric profiles from rotational analysis of CO_2 lines in atmospheric trace molecule spectroscopy/ATLAS 1infrared solar occultation spectra", J. Geophys. Res., **100**, D2, pp 3107-3117, 1995.
6. V.S. Kumar, Y.B. Kumar, K. Raghunath, P.B. Rao, M. Krishnaiah, K. Mizutani, T. Aoki, M. Yasui, and T. Itabe, "Lidar measurements of mesospheric temperature inversion at low latitude", Annales Geophysicae, **19**, pp 1039-1044, 2001.